NATIONAL ADVISORY COMMITTEE FOR AERONAUTICS

# WARTIME REPORT

ORIGINALLY ISSUED
March 1945 as
Confidential Bulletin L5C09

## NOTE ON COMPRESSIBILITY EFFECTS ON DOWNWASH AT THE TAIL AT SUBCRITICAL SPEEDS

By Jack N. Nielsen and Harold H. Sweberg

Langley Memorial Aeronautical Laboratory
Langley Field, Va.



WASHINGTON

NACA CB No. L5C09 [redacted]

NATIONAL ADVISORY COMMITTEE FOR AERONAUTICS

CONFIDENTIAL BULLETIN

# NOTE ON COMPRESSIBILITY EFFECTS ON DOWNWASH AT THE TAIL AT SUBCRITICAL SPEEDS

By Jack N. Nielsen and Harold H. Sweberg

## SUMMARY

Calculations have been made to show the magnitude of the compressibility effects on the downwash at the tail at subcritical speeds. Experimental results of tests of two airplane models are included to give some verification of the theory.

The calculations showed that the effects of compressibility on the span load distribution along the wing and on the downwash angle at the tail are small for constant values of the lift coefficient. The experimental results confirmed these calculations.

## INTRODUCTION

A rational solution for the problem of longitudinal stability at high speeds requires a knowledge of the effects of compressibility on the downwash in the region of the horizontal tail surface. Studies of this problem for speeds below the critical have been reported by Husk in reference 1 and by Goldstein and Young in reference 2. In reference 1 the downwash at the tail is assumed to be unaffected by increases in Mach number for constant values of the lift coefficient. In reference 2, on the basis of the Glauert-Prandtl theory, the downwash is found to decrease slightly with increases in Mach number for constant values of the lift coefficient and span loading. No experimental verifications of the conclusions stated in these reports are given.

The present paper presents theoretical calculations, based on the methods of reference 2, to show the magnitude of the compressibility effects on downwash and gives some experimental verification of the theory. Calculations

[redacted]

have been made to obtain the span load distributions along the wing and the average downwash angles at the tail of a typical pursuit airplane for a range of lift coefficient and Mach number. Wind-tunnel test data showing the effect of compressibility on the average downwash angles at the tail have also been included for two airplane models.

## SYMBOLS

| | |
|---|---|
| $C_L$ | airplane lift coefficient (horizontal tail removed) |
| $c_{l_b}$ | basic section lift coefficient $(C_L = 0)$ |
| $c_{l_a}$ | additional section lift coefficient |
| $M_o$ | free-stream Mach number |
| c | chord |
| b | wing span |
| y | distance outboard along span from wing center line |
| x | distance from wing quarter-chord line to elevator hinge line |
| $\epsilon$ | downwash angle, degrees |
| $\alpha$ | angle of attack, degrees |
| $\alpha_{(\alpha_t=0^\circ)}$ | airplane angle of attack for zero angle of attack of tail, degrees |
| $i_t$ | angle of incidence of stabilizer relative to airplane reference line |

## THEORETICAL CALCULATIONS

The effects of compressibility on the downwash at the tail may be considered the result of two factors:

[redacted]

the change in span loading along the wing and the change in downwash for a given span loading. Methods for calculating both these changes are given in reference 2 in which the Glauert-Prandtl theory of compressible flow is used. According to reference 2, the span loading for any Mach number may be approximated by using the slope of the lift curve for compressible flow in the equation of the lifting-line theory (reference 3). The downwash at a distance x behind the lifting line may now be determined by the methods of reference 4 for incompressible flow except that the distance of the tail behind the lifting line is increased by the ratio $1/\sqrt{1 - M_o^2}$.

In order to show the magnitude of the compressibility effects, calculations have been made in which the aforementioned methods are used to determine the span loading along the wing and the resultant downwash at the tail of a high-speed pursuit airplane. The distributions of twist and chord along the wing shown in figure 1, which correspond approximately to the distributions for a modern pursuit airplane, were used for the calculations. The twist at the inboard sections is used to increase the critical speed of the wing-fuselage juncture.

Span load distribution.- The load distribution along the span has been determined in two parts. The first part, which is due to wing twist, is the load distribution at zero lift and is referred to as the basic load distribution. This distribution has been calculated by the method of reference 5 using ten harmonics for the circulation because of the sharp break in the wing twist distribution. For these calculations, the slope of the section lift curve was taken as $5.67/\sqrt{1 - M_o^2}$ per radian. Basic load distributions along the wing span are given in figure 2 for Mach numbers of 0 and 0.8. Although the slope of the section lift curve for $M_o = 0.8$ is increased 66 percent over that for $M_o = 0$, the ordinates of the basic-load-distribution curve show an average increase of only about 20 percent; that is, the effect of the increased slope of the section lift curve is diminished to a large extent as a result of the small span within which the twist is effected.

The second part of the load distribution is that due to the untwisted wing operating at a given lift coefficient and is referred to as the additional load distribution.

[redacted]

This distribution has been taken from reference 6 for a lift coefficient of 1.0 and is shown plotted in figure 3 for Mach numbers of 0 and 0.8. The additional load distribution is seen to be almost unaffected by compressibility. This result depends on the wing plan form. For an elliptical wing, the additional load distribution remains elliptical regardless of the slope of the section lift curve. For other than elliptical wings, increasing the slope of the section lift curve causes the additional load distribution to become more nearly elliptical but the effect will normally be small, as in the present case.

The additional load distribution for lift coefficients other than 1.0 may be obtained simply by multiplying the ordinates in figure 3 by the lift coefficient. Since the total load distribution is obtained by adding the additional load distribution to the basic load distribution, it may be concluded that below the critical speed the total load distribution for a given lift coefficient will also be changed very little by compressibility. Span load distributions for elliptical wings of approximately zero aerodynamic twist given in reference 7 and calculated from experimental section-lift-curve slopes show very small changes with Mach number up to the critical speed.

Downwash at tail.- By using the compressible-flow span load distributions, calculations have been made by the method of reference 4 of the average downwash across the tail span for a range of lift coefficient and Mach number. For these calculations, the angle of attack for zero lift was assumed to be independent of Mach number and the distance of the tail behind the lifting line was taken as $0.95\frac{b}{2}\sqrt{1 - M_o^2}$. The downwash angles were calculated at three points along the tail semispan and the results were averaged to obtain the average downwash angle at the tail. These results are shown in figure 4.

The variations of downwash angle with Mach number for constant values of lift coefficient (fig. 4) are small. For low values of the lift coefficient, the changes in downwash angle with Mach number are inappreciable except at very high values of the Mach number (above about $M_o = 0.7$). At the high lift coefficients, the downwash decreased slightly with increasing Mach number up to a Mach number of about 0.7. At Mach numbers

[redacted]

higher than about 0.7, the downwash angle decreases more rapidly than at the lower Mach numbers.

The decrease in downwash angle with Mach number for constant lift coefficient results from two effects: (1) the distance from the lifting line to the tail, used for the downwash computations, increases with increasing Mach number, and (2) the tail moves farther above the wake since, for a given lift coefficient, the angle of attack decreases as the Mach number increases.

It has already been remarked that increasing Mach number causes the span load distribution to become more elliptical. For a highly tapered wing, which has proportionately more trailing vorticity inboard than an elliptical wing, the effect tends to cause a reduction in downwash; for a rectangular wing, which has proportionately more trailing vorticity outboard, the effect tends to cause an increase in downwash. In either case, as for the load distribution itself, computations show that the effect is small.

Although the change in downwash angle with Mach number for constant lift coefficient has been shown to be small, it does not follow that the change in the longitudinal stability characteristics will be small. In particular, the angle of attack of the wing for a given lift coefficient will decrease with increasing Mach number because of the increase in the slope of the lift curve and, as a result, the angle of attack of the tail for the same lift coefficient will decrease a corresponding amount. This decrease in tail angle of attack for a given lift coefficient will cause an increase in airplane pitching-moment coefficient and a rearward shift of the neutral point. Because of the different aspect ratios of the wing and tail, furthermore, a disproportionate increase in the wing and tail lift-curve slopes will occur that also causes a shift of the neutral point.

## EXPERIMENTAL RESULTS

An analysis has been made of wind-tunnel test data obtained at high Mach numbers to verify experimentally the theory and calculations presented in the preceding section. The data were obtained from tests of complete

models of the P-51B and XP-58 airplanes in the Ames 16-foot high-speed wind tunnel. Downwash angles were computed from the results of pitching-moment measurements with the horizontal tail set at several angles of incidence and with the horizontal tail removed. The intersection of the pitching-moment curves for this model with the tail on and with the tail off gave the airplane angle of attack for which the tail angle of attack is zero. The downwash angles were then computed from the relation

$$\epsilon = \alpha_{(\alpha_t=0^\circ)} + i_t$$

where $\alpha_{(\alpha_t=0^\circ)}$ is the airplane angle of attack for zero tail angle of attack and $i_t$ is the stabilizer incidence, relative to the airplane reference axis.

Inasmuch as the wind-tunnel test data were corrected by incompressible-flow methods, it was necessary to investigate the effect of compressibility on the wind-tunnel wall corrections. The effect of the tunnel walls is to cause an increment of upwash at the wing and an additional increment of upwash at the tail. These increments necessitate a correction to the airplane angle of attack and tail-on pitching-moment coefficient. Goldstein and Young (reference 2) showed that the correction to the airplane angle of attack is unchanged for compressible flow but that the correction to the tail-on pitching-moment coefficient must be adjusted for compressibility. This adjustment is made by assuming that the tail is at a distance $x/\sqrt{1 - M_o^2}$ instead of a distance $x$ behind the wing quarter-chord line.

The variation of the downwash angle with Mach number for several values of the lift coefficient is given in figure 5 for the P-51B airplane model. In order to show the limits of the subcritical region and also to facilitate the use of the data given in figure 5, curves of lift coefficient against Mach number for several angles of attack are given in figure 6. Similar downwash and lift data are presented in figures 7 and 8 for the XP-58 airplane model. For both airplane models some downwash exists at zero lift (between 1° and 2°). No definite reason can be given for this apparent discrepancy; it may

[redacted]

result, however, from either the wing twist or inaccuracies in the tail settings, or from both. Although the absolute magnitude of the downwash angles may be in error, the variation of the downwash angle with Mach number is considered accurate.

The results plotted in figures 5 and 7 show that at low lift coefficients, which correspond to high-speed flight, the change in downwash angle with Mach number is negligible. At the high lift coefficients, some change in the downwash angle with Mach number occurs. This change is small for the case of the P-51B airplane model but amounts to about 0.5° for the XP-58 airplane model. The experimental results, in general, agree with the theory in that the variation of downwash angle with Mach number at constant lift coefficient is relatively small.

## DOWNWASH AT SUPERCRITICAL SPEEDS

Although the present paper is primarily concerned with the downwash at subcritical speeds, a few remarks regarding the downwash at supercritical speeds should be made. Evidence is available (references 7 and 8) which shows that large changes in span loading may occur at supercritical speeds. The changes in span loading may cause appreciable changes in the downwash at the tail. If flow breakdown due to shock occurs first at the inboard wing sections because of their thickness or because of wing-fuselage interference, there will be a shift of the load outboard and a consequent reduction in the downwash at the tail. Unfortunately, these effects are not well understood because theory has not been developed and wind-tunnel test data are insufficient at supercritical speeds for which conditions the wind-tunnel tare and interference corrections are not well understood at present.

## CONCLUDING REMARKS

Theoretical calculations have shown that the effect of compressibility at subcritical speeds on the span load distribution along the wing and on the downwash angle at the tail is small for constant values of the lift coefficient. Experimental results of the downwash variation

[redacted]

with Mach number for two airplane models confirmed these calculations. At supercritical speeds, however, large changes in the span loading and in the downwash for constant values of the lift coefficient may occur.

Langley Memorial Aeronautical Laboratory
National Advisory Committee for Aeronautics
Langley Field, Va.

REFERENCES

1. Husk, D. I.: Compressible Flow behind a Wing. Aircraft Engineering, vol. XIV, no. 160, June 1942, p. 160.

2. Goldstein, S., and Young, A. D.: The Linear Perturbation Theory of Compressible Flow, with Applications to Wind-Tunnel Interference. R. & M. No. 1909, British A.R.C., 1943.

3. Glauert, H.: The Elements of Aerofoil and Airscrew Theory. Cambridge Univ. Press, 1926, p. 139.

4. Silverstein, Abe, and Katzoff, S.: Design Charts for Predicting Downwash Angles and Wake Characteristics behind Plain and Flapped Wings. NACA Rep. No. 648, 1939.

5. Pearson, H. A.: Span Load Distribution for Tapered Wings with Partial-Span Flaps. NACA Rep. No. 585, 1937.

6. Anderson, Raymond F.: Determination of the Characteristics of Tapered Wings. NACA Rep. No. 572, 1936.

7. Boshar, John: The Determination of Span Load Distribution at High Speeds by Use of High-Speed Wind-Tunnel Section Data. NACA ACR No. 4B22, 1944.

8. Whitcomb, Richard T.: The Relation between Spanwise Variations in the Critical Mach Number and Spanwise Load Distributions. NACA CB No. L4L07, 1944.

[redacted]

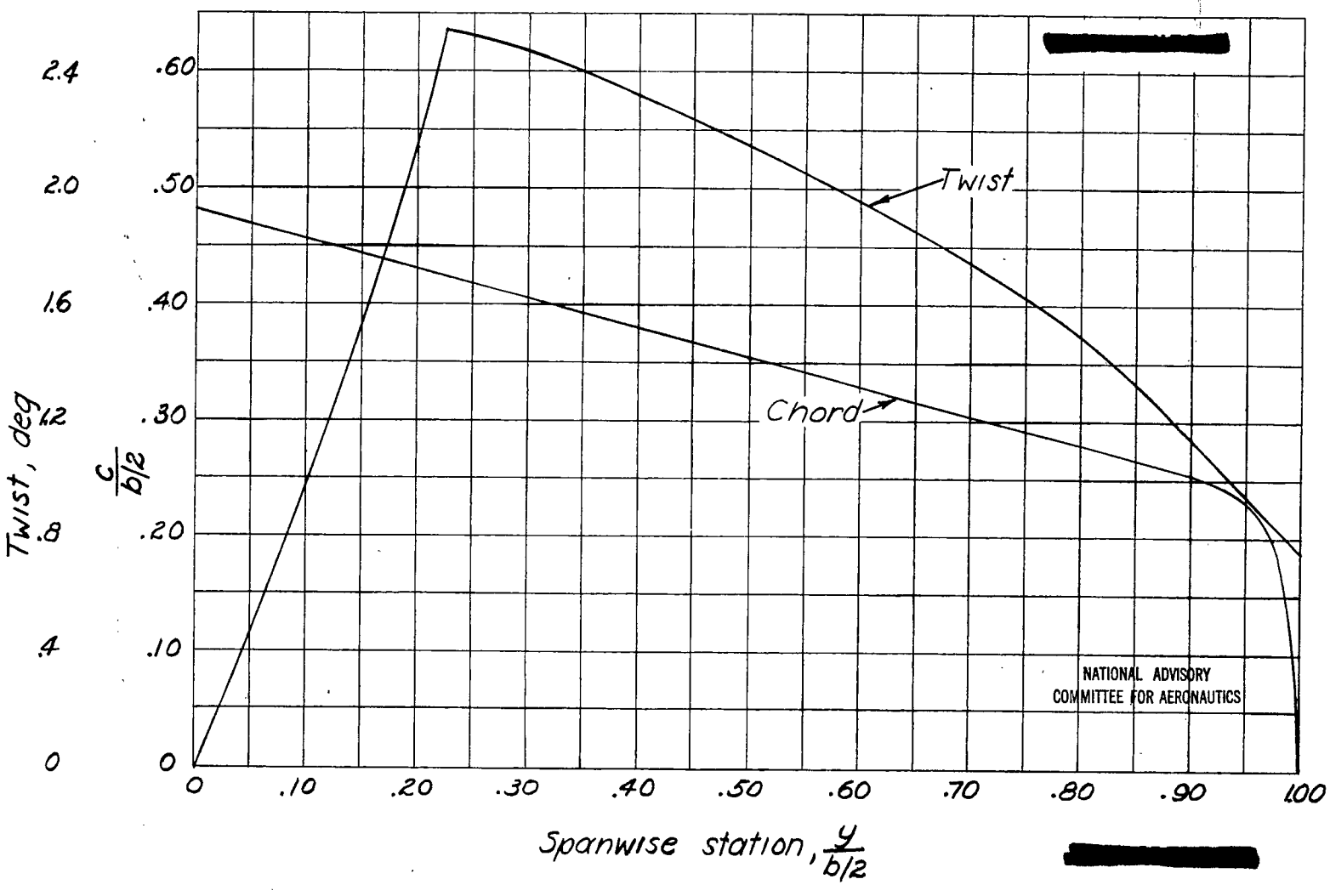


Figure 1. - Distribution of twist and chord along wing, used for span loading and downwash calculations.

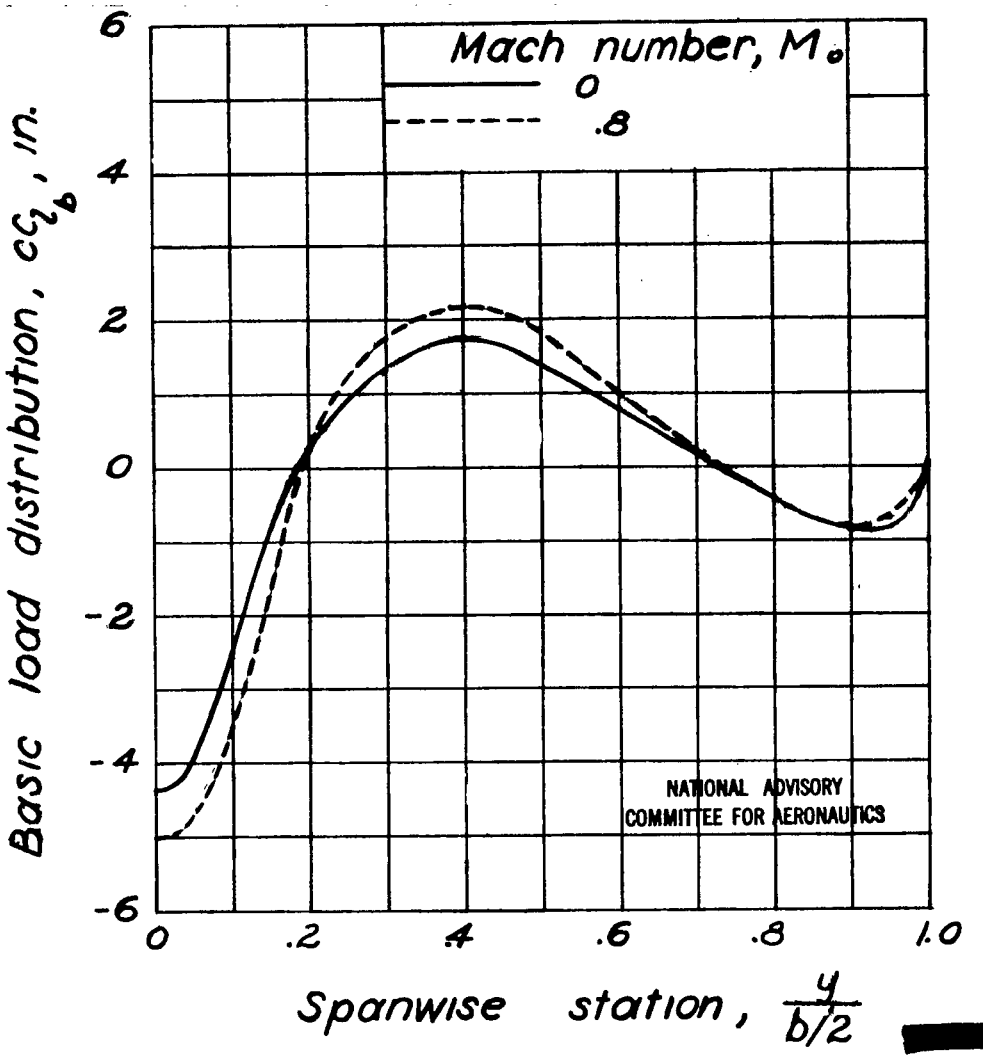


Figure 2.- Effect of Mach number on the basic span load distribution.

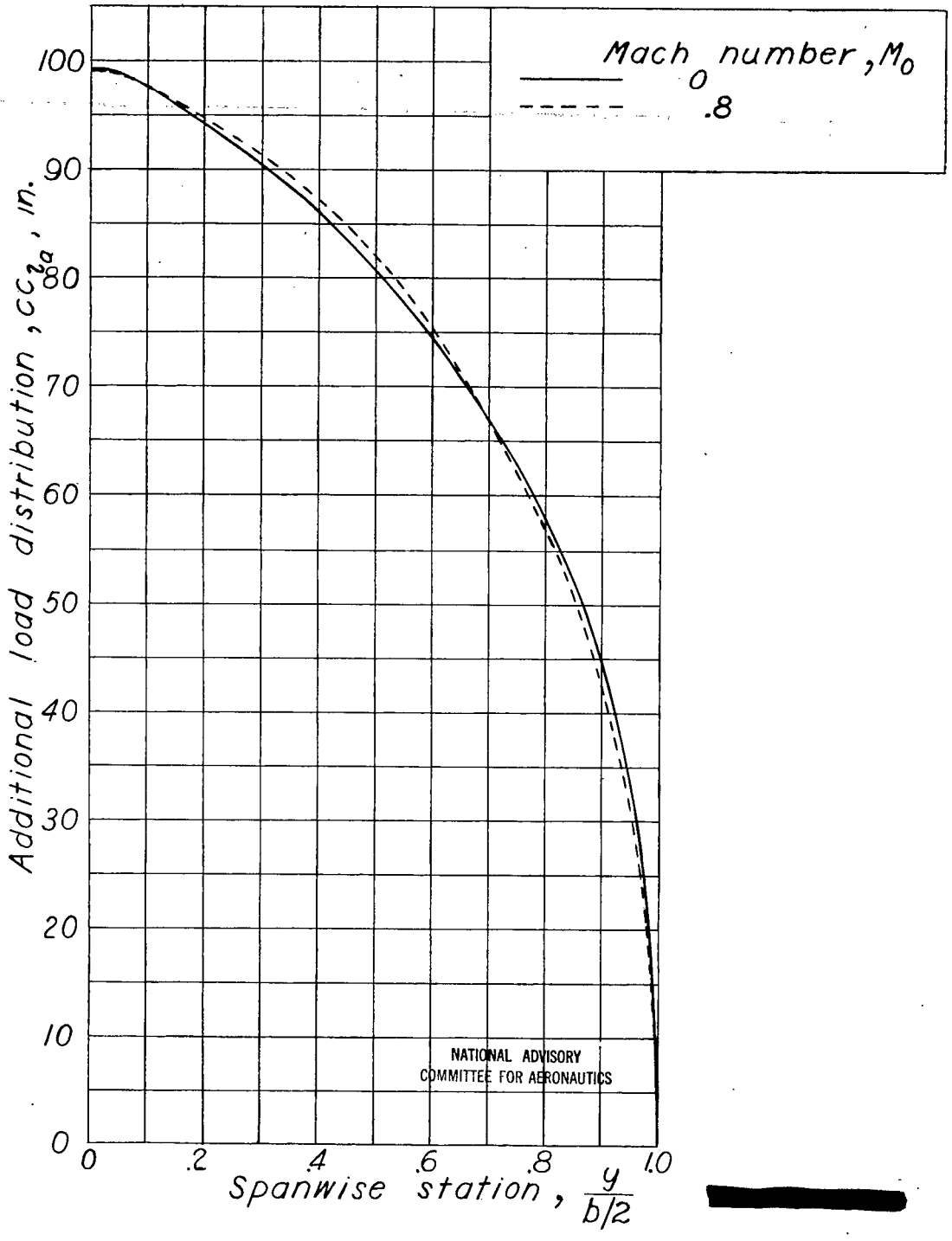


Figure 3.- Effect of Mach number on the additional span load distribution.

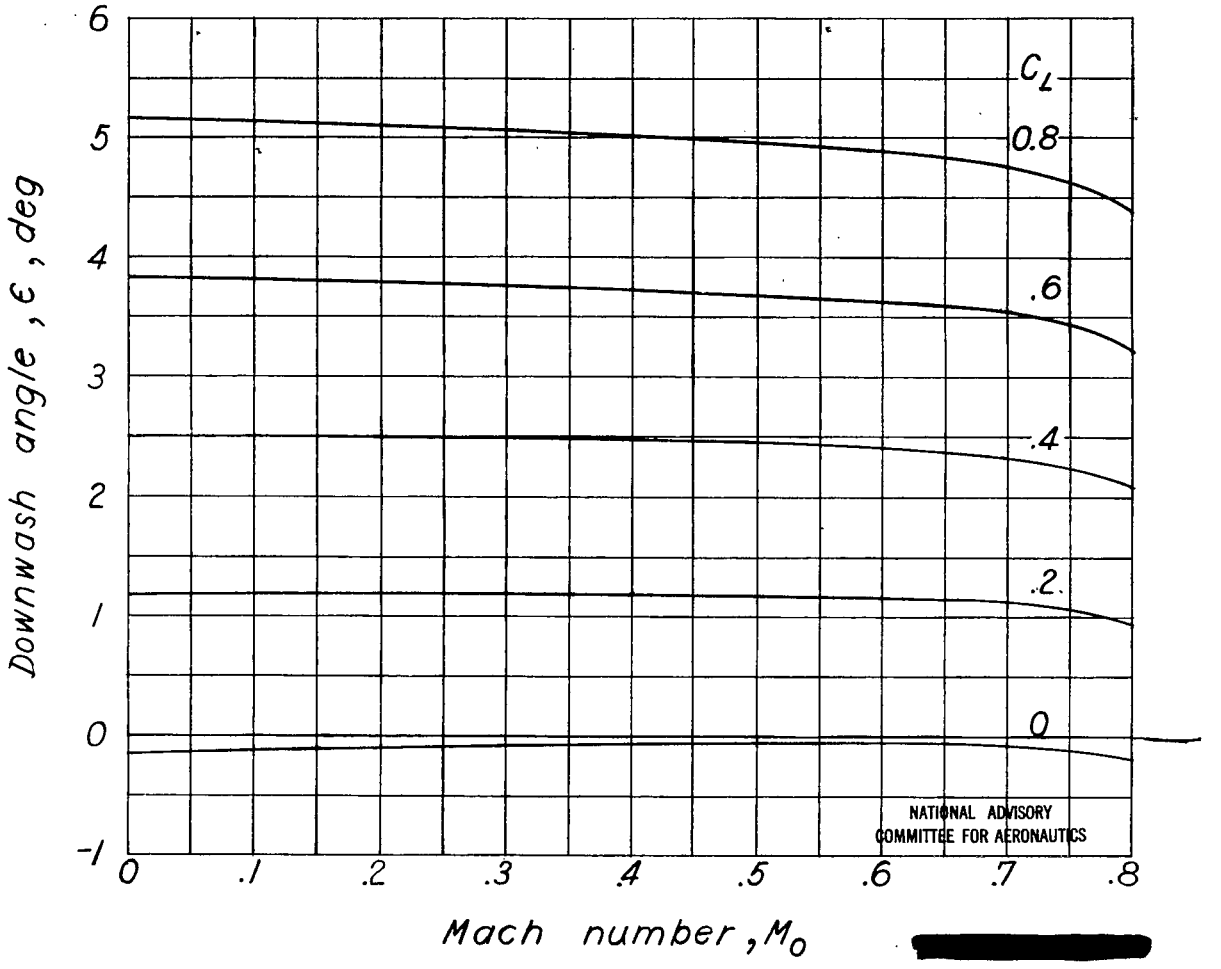


Figure 4.- Calculated variation of the downwash angle with Mach number for constant values of the lift coefficient.

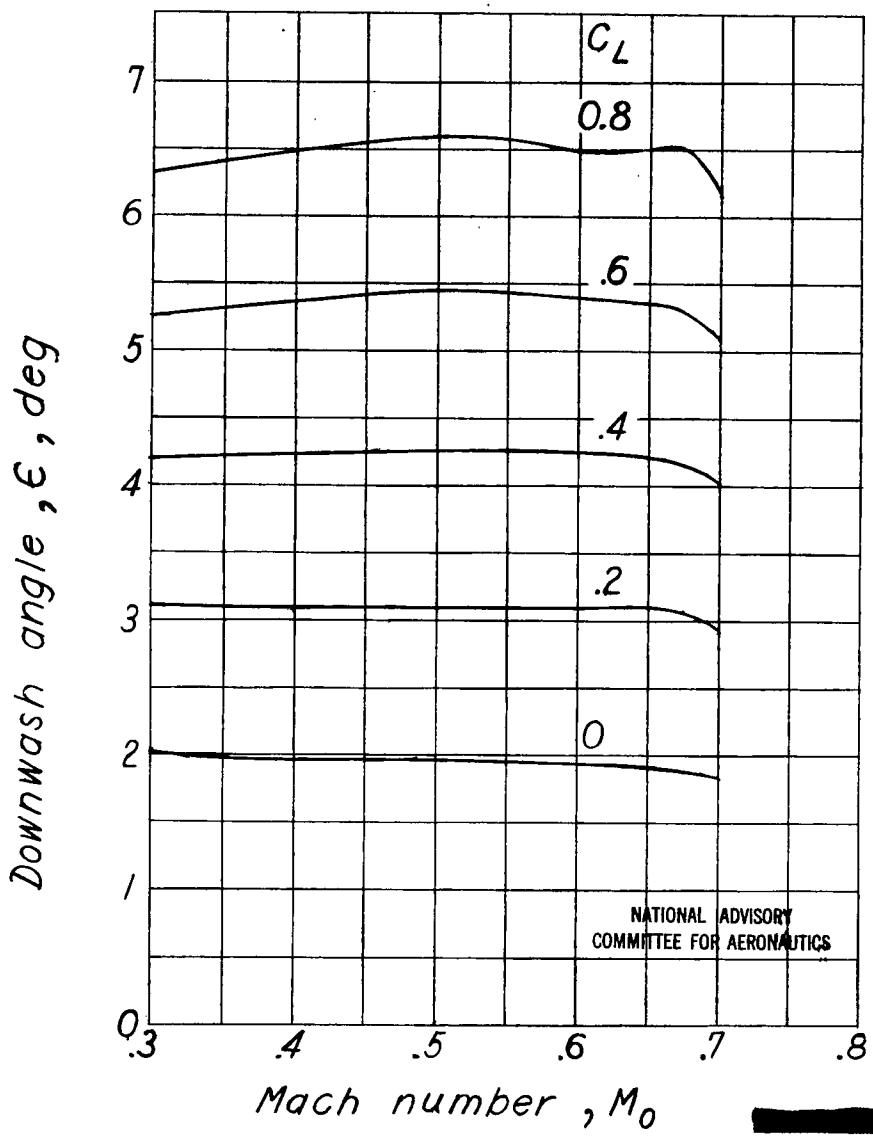


Figure 5.—Experimental variation of the downwash angle with Mach number for constant values of the lift coefficient, P-51B airplane model.

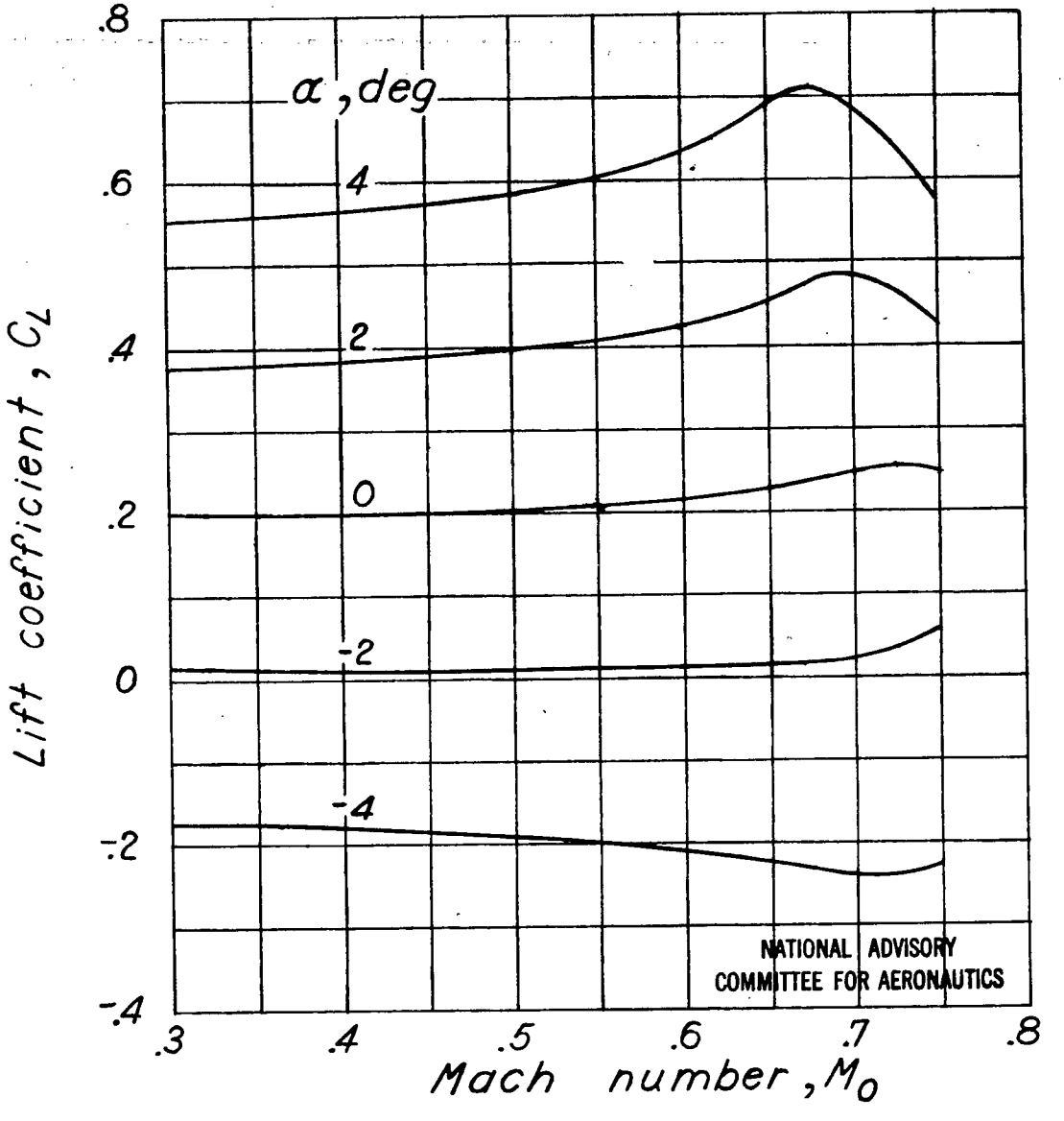


[redacted]

Figure 6.- Variation of lift coefficient with Mach number for the P-51B airplane model.

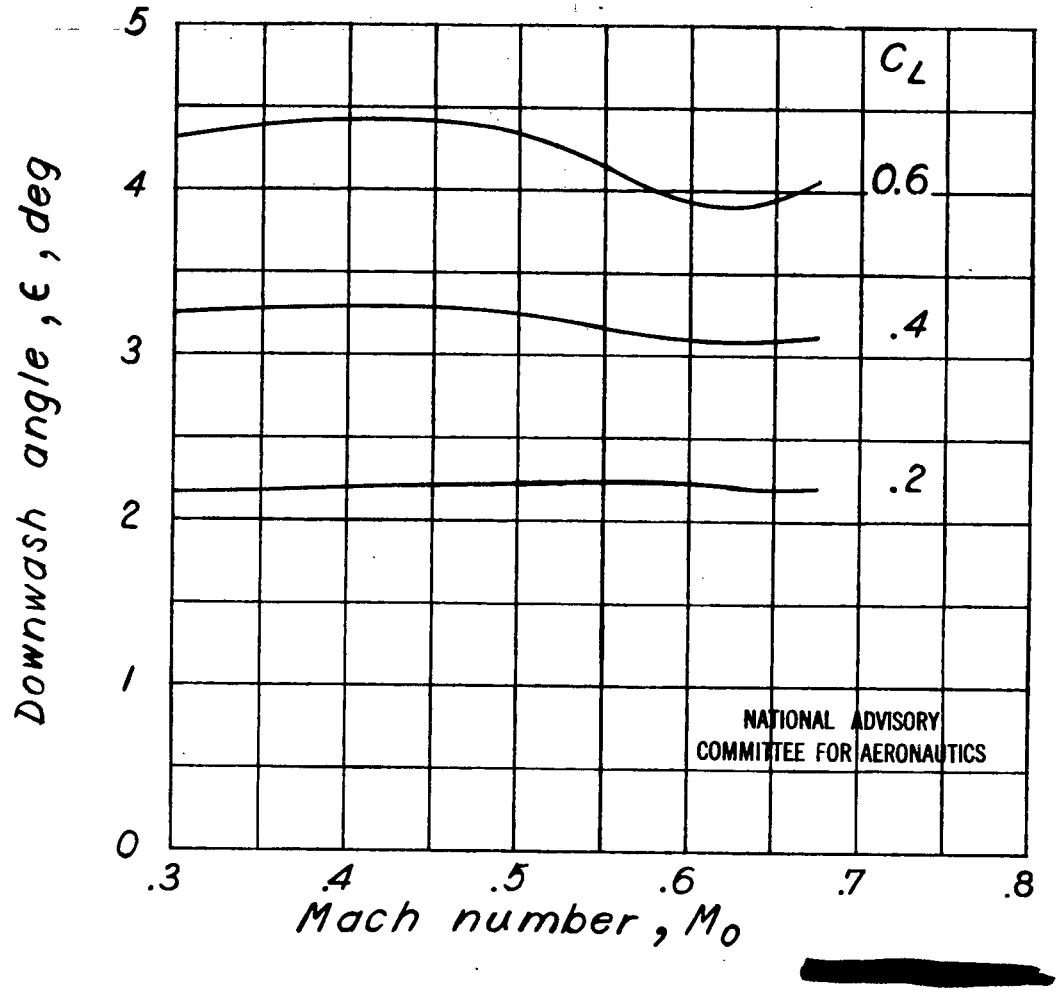


Figure 7.- Experimental variation of the downwash angle with Mach number for constant values of the lift coefficient; XP-58 airplane model.

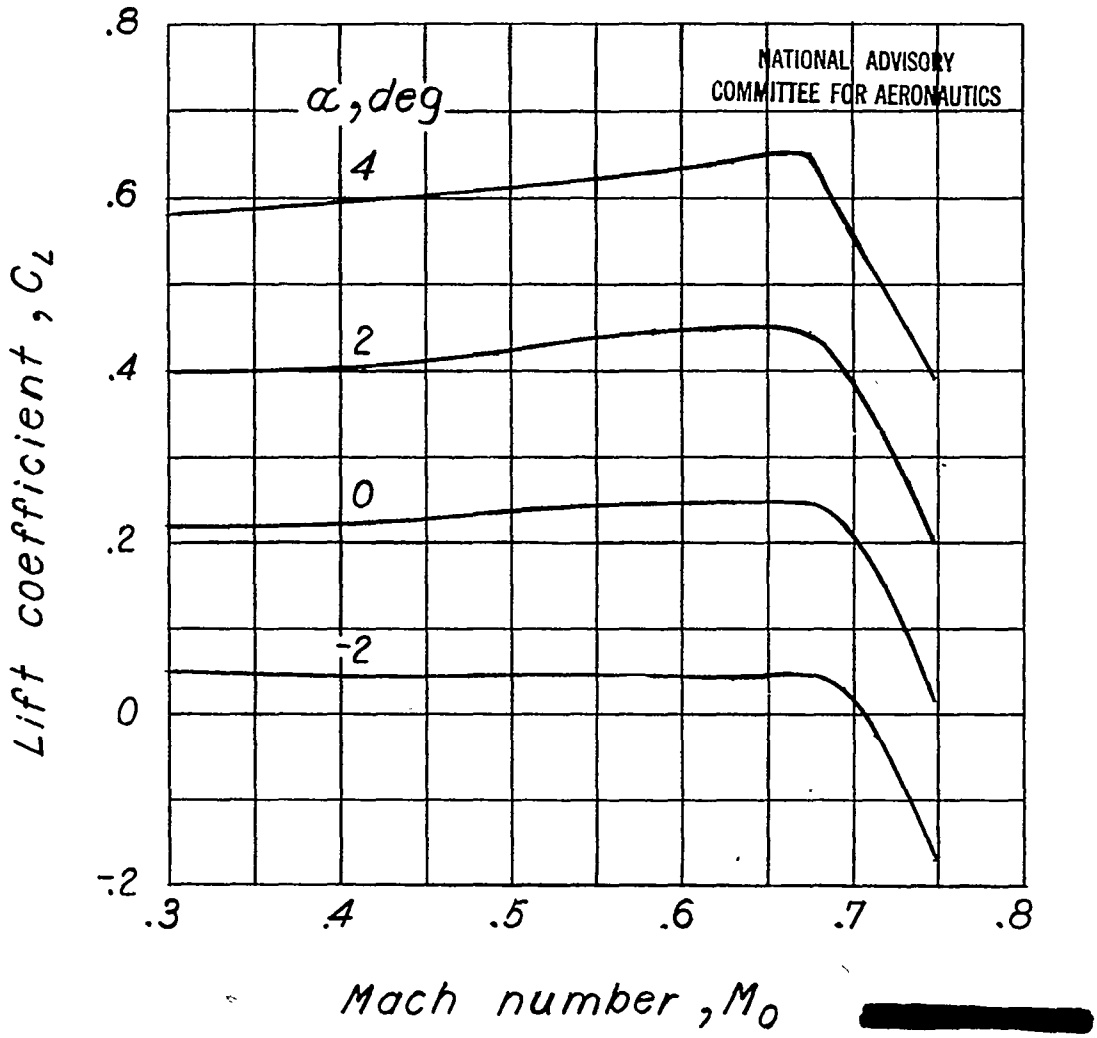


Figure 8.- Variation of lift coefficient with Mach number for the XP-58 airplane model.